Vegetation patterns associated with nutrient availability and supply in high-elevation tropical Andean ecosystems

Armando Molina[1,2], Veerle Vanacker[3], Oliver Chadwick[4], Santiago Zhiminaicela[5], Marife Corre[1], and Edzo Veldkamp[1]

[1]Soil Science of Tropical and Subtropical Ecosystems, Faculty of Forest Sciences and Forest Ecology, University of Göttingen, Göttingen, Germany.

[2]Facultad de Ciencias Agropecuarias, Universidad de Cuenca, Campus Yanuncay, Cuenca, Ecuador.

[3]Earth and Life Institute, Centre for Earth and Climate Research, University of Louvain, 3 Place Louis Pasteur, B-1348 Louvain-la-Neuve, Belgium.

[4]Department of Geography, University of California, Santa Barbara, Santa Barbara, CA 93106-4060, USA.

[5]Subgerencia de Operaciones, Agua Potable y Saneamiento, Empresa Pública Municipal de Telecomunicaciones, Agua Potable, Alcantarillado y Saneamiento de Cuenca (ETAPA EP), Cuenca, Ecuador.

Correspondence to: A. Molina (Armando.molinav@ucuenca.edu.ec). Facultad de Ciencias Agropecuarias, Universidad de Cuenca, Campus Yanuncay, Cuenca, Ecuador. V.Vanacker (veerle.vanacker@uclouvain.be). Earth and Life Institute, University of Louvain, Louvain-la-Neuve, Belgium.

Abstract.

Plants absorb nutrients and water through their roots, and modulate soil biogeochemical cycles. The mechanisms of water
20   and nutrient uptake by plants depend on climatic and edaphic conditions, as well as the plant root system. Soil solution is the
medium in which abiotic and biotic processes exchange nutrients, and nutrient concentrations vary with the abundance of
reactive minerals and fluid residence times. High-altitude ecosystems of the tropical Andes are presumably interesting to
study the association between vegetation, soil hydrology and mineral nutrient availability at the landscape scale. First of all,
because of low rock-derived nutrient stocks in intensely weathered volcanic soils, biocycling of essential nutrients by plants
25   is expected to be important for plant nutrient acquisition. Second, the ecosystem is characterised by strong spatial patterns in
vegetation type and density at the landscape scale, and hence optimal to study soil-water-vegetation interactions. Third, the
area is characterised by high carbon stocks but low rates of organic decomposition that might vary with soil hydrology, soil
development and geochemistry, all interconnected with vegetation. The páramo landscape forms a vegetation mosaic of
bunch-grasses, cushion-forming plants and forests. In the nutrient-depleted nonallophanic Andosols, the plant rooting depth
30   varies with drainage and soil moisture conditions. Rooting depths were shallower in seasonally waterlogged soils under
cushion plants and deeper in well-drained soils under forest and tussock grasses (> 100 cm). Vegetation composition is a
relevant indicator of rock-derived nutrient availability in soil solutions. The soil solute chemistry revealed patterns in plant
available nutrients that were not mimicking the distribution of total rock-derived nutrients nor the exchangeable nutrient
pool, but clearly resulted from strong biocycling of cations and removal of nutrients from the soil by plant uptake or deep
35   leaching. Soils under cushion plants showed solute concentrations of Ca, Mg and Na of about 3 times higher than forest and
tussock grasses. Differences were even stronger for dissolved Si with solute concentrations that were 16 times higher than
forest and 6 times higher than tussock grasses. Amongst the macronutrients derived from lithogenic sources, P was a limiting
nutrient with very low solute concentrations (< 1 μM) for all three vegetation types. In contrast K showed greater solute
concentrations under forest soils with values that were 2 to 3 times higher than under cushion-forming plants or tussock
40   grasses. Our findings have important implications for future management of Andean páramo ecosystems where vegetation
type distributions are dynamically changing as a result of warming temperatures and land use change. Such alterations may
not only lead to changes in soil hydrology and solute geochemistry but also to complex changes in weathering rates and
solute export downstream with effects on nutrient concentrations in Andean rivers and high-mountain lakes.

1 Introduction

45 Plants absorb nutrients and water through their roots, and modulate soil biogeochemical cycles (Kelly et al., 1998; Jackson et al., 2002; Amundson et al., 2021). The availability of soil nutrients regulates terrestrial primary productivity (Chadwick et al., 1999; Vitousek, 2004; White et al., 2012; Uhlig et al., 2020). In young ecosystems, plant-essential mineral nutrients such as calcium (Ca), potassium (K), magnesium (Mg), phosphorus (P), and silica (Si) are derived from mineral weathering of rock and soil (Chadwick et al., 1999; Hedin et al., 2003; Dixon et al., 2016). When the nutrient supply from lithogenic sources

50 declines, biocycling of essential nutrients by plants becomes more important (Landeweert et al., 2001; Vitousek et al., 2003). Thus nutrient acquisition and water uptake by plant roots drive the circulation of water and dissolved nutrients within the soil mantle (Uhlig et al., 2017; Rempe and Dietrich, 2018), while litterfall, root decay, and decomposition release nutrients and make them bioavailable again (Hobbie, 1992; Amundson et al., 2007).

55 Soil solution is the medium in which abiotic and biotic processes exchange nutrients (Niemenen et al., 2013; Olshansky et al., 2019). Nutrient concentrations in shallow soil water are recharged by biological processes and vary seasonally with plant growth cycles (White et al., 2012) that depend on temperature and rainfall. Biologically essential nutrient concentrations are often highest in the upper soil horizons, a result of mineralization and deposition processes (Jobbágy and Jackson, 2001, 2004). Atmospheric deposition including occult deposition from fog and clouds can further contribute to replenish soil nutrient stocks

60 of e.g. calcium (Hofhansl et al., 2011; Ping et al., 2013). Nutrient concentrations in deeper soil water increase with depth, a result of mineral weathering and exchange processes, due to the abundance of reactive minerals and longer fluid residence times (Brantley and White, 2009; White et al., 2012).

The mechanisms of water and nutrient uptake by plants depend on climatic and edaphic conditions (Porder and Chadwick,

65 2009), as well as the plant root system, and rooting depth (Schenk and Jackson, 2002). Plants typically take up soil water using shallow roots, although deep roots can play a key role in acquiring water and nutrients from deeper soil horizons and redistribute them to shallower horizons, particularly during drought (Brantley et al., 2017; Hasenmueller et al., 2017; Dawson et al., 2020). In well-drained aerated upland, soils and plant rooting typically follow infiltration depth, whereas in waterlogged anaerobic soils, often shallow roots develop (Fan et al., 2017). Plant rooting depth can, in turn, influence soil hydrology through

70 water uptake and transpiration losses (Cramer et al., 2008), chemical weathering (Canadell et al., 1996; Rempe and Dietrich, 2018), and regulate long-term carbon storage and soil nutrient distributions (Jackson et al., 2000).

Despite the importance of biological and geochemical processes in regulating nutrient availability in terrestrial ecosystems, few studies have addressed the role of vegetation communities and soil hydrology in influencing soil nutrient availability

75 which is a research gap. High Andean tropical ecosystems provide a good opportunity to study the association between vegetation patterns, soil hydrology and soil nutrient availability: the climate, parent material, and soil age can be held constant

at the landscape scale, while the vegetation and soil hydrology can vary greatly from the hilltops to the valley bottoms. High-altitude grassland ecosystems of the tropical Andes, known as páramo ecosystems, have average air temperatures ranging between 2 and 10 °C. Seasonal variations in air temperature are small, but strong diurnal temperature oscillations occur (Bader and Ruijten, 2008). Mean annual precipitation is regionally variable, and between 500 and 3000 mm. Water is rarely limiting plant growth, and the evaporative demand and soil microbial decomposition rates are low due to the frequent presence of cloud and fog (Ramsay, 1992; Tonneijck et al., 2010). In periods with high solar radiation, wind speed and low cloudiness, air and soil temperatures can quickly rise leading to short moments of high evaporative demand (Páez-Bimos et al., 2023; Carabajo-Hidalgo et al., 2023). Moderate to highly weathered uniform soils (Podwojewski and Poulenard, 2000; Molina et al., 2019) are prevalent, and they are rich in organic matter content. Carbon sequestration is particularly remarkable leading to total carbon stocks of 17 kg C m^{-2} for the top 30 cm of soil (Minaya et al., 2016) and 53 kg C m^{-2} in the upper 100 cm soil (Tonneijck et al., 2010). Páez-Bimos et al. (2023) reported particularly high concentrations in dissolved organic carbon in soil solutes (up to 47.3 ± 2.3 mg L^{-1} in topsoil samples) leading to mean annual dissolved organic carbon fluxes of 17.4 g m^{-2} yr^{-1} despite relatively low water fluxes. High Andean rivers have a particular stream load as their dissolved load exceeds the suspended solid load during normal hydrological years (Tenorio et al., 2018). The elevated dissolved organic carbon concentrations cause extra acidy in water with consequences on the aquatic ecology of rivers and high-mountain lakes (Mosquera et al., 2022).

The overall objective of this study is to analyse potential association between vegetation, soil hydrology and mineral nutrient availability at the landscape scale. It is part of a larger group of studies on soil-water-vegetation interactions in tropical volcanic ecosystems that used the same sampling scheme for maximum inter-site comparability (Molina et al., 2019; Páez-Bimos et al., 2022). The site in the southern Ecuadorian Andes is underlain by andesitic parent material, and soils experience only limited input of Holocene distal tephra (Rodbell et al., 2002). External soil nutrient input from e.g. dust and ocean-salt aerosols can be assumed to be minimal. We measured nutrients over the course of one hydrological year in soil pore water solutions, under different combinations of vegetation, soil moisture and drainage conditions to address the following research questions: (1) How does vegetation regulate soil moisture, drainage and soil development? (2) How are soil moisture conditions related to the availability of rock-derived nutrients (Ca, K, Mg, Na, P and Si) in the soil solution? and (3) How does vegetation influence the relative availability of nutrients? We posit here that soil drainage and moisture conditions, and rock-derived nutrient availability in soil solutions vary with vegetation type at the landscape scale. The study is based on a new dataset containing data on soil solution chemistry and soil water potential collected over a full hydrological year, and was complemented with data on soil bulk chemistry and soil hydraulics.

2 Site description

Our study was carried out at the Cuevas catchment (4.2 km²), located in a grassland (or so-called páramo) ecosystem on the western Cordillera in southern Ecuador, about 30 km southwest of the city of Cuenca (3°01'50" S, 79°17'59" W, Molina et

al., 2019). Altitudes range from 3608 to 3960 m asl, with gently sloping (< 12%) valley bottoms and steeper slopes (12-25%)
110 on the hillsides. The glaciated landscape was shaped during the Pleistocene giving rise to frequently observed glacial features
such as moraines, U-shaped valleys and glacial lakes (Jantz and Behling, 2012). The site is part of an area that is protected by
the public drinking water company (ETAPA EP). This páramo ecosystem has an udic moisture regime and an isomesic
temperature regime (Poulenard et al., 2003; Buytaert et al., 2005). The annual rainfall (1998-2013 period) averaged 911 mm
at the Soldados meteorological station (3500 m a.s.l., ETAPA EP), and exhibits a bimodal regime (Mora and Willems, 2012).
115 There is also a continuous moisture input from clouds and fog. The air temperature is seasonally constant with a mean annual
air temperature of about 8°C at 2.5 m above the terrain (ETAPA EP). Although the mean temperature shows little seasonal
variation, there are strong diurnal variations with a maximum temperature of 18 °C during the day and a minimum temperature
of 1°C during the night. Because of the low temperature and year-round air humidity, the evapotranspiration is estimated at 45
to 60% of the total annual rainfall (Carrillo-Rojas et al., 2019; Lazo et al., 2019).

120
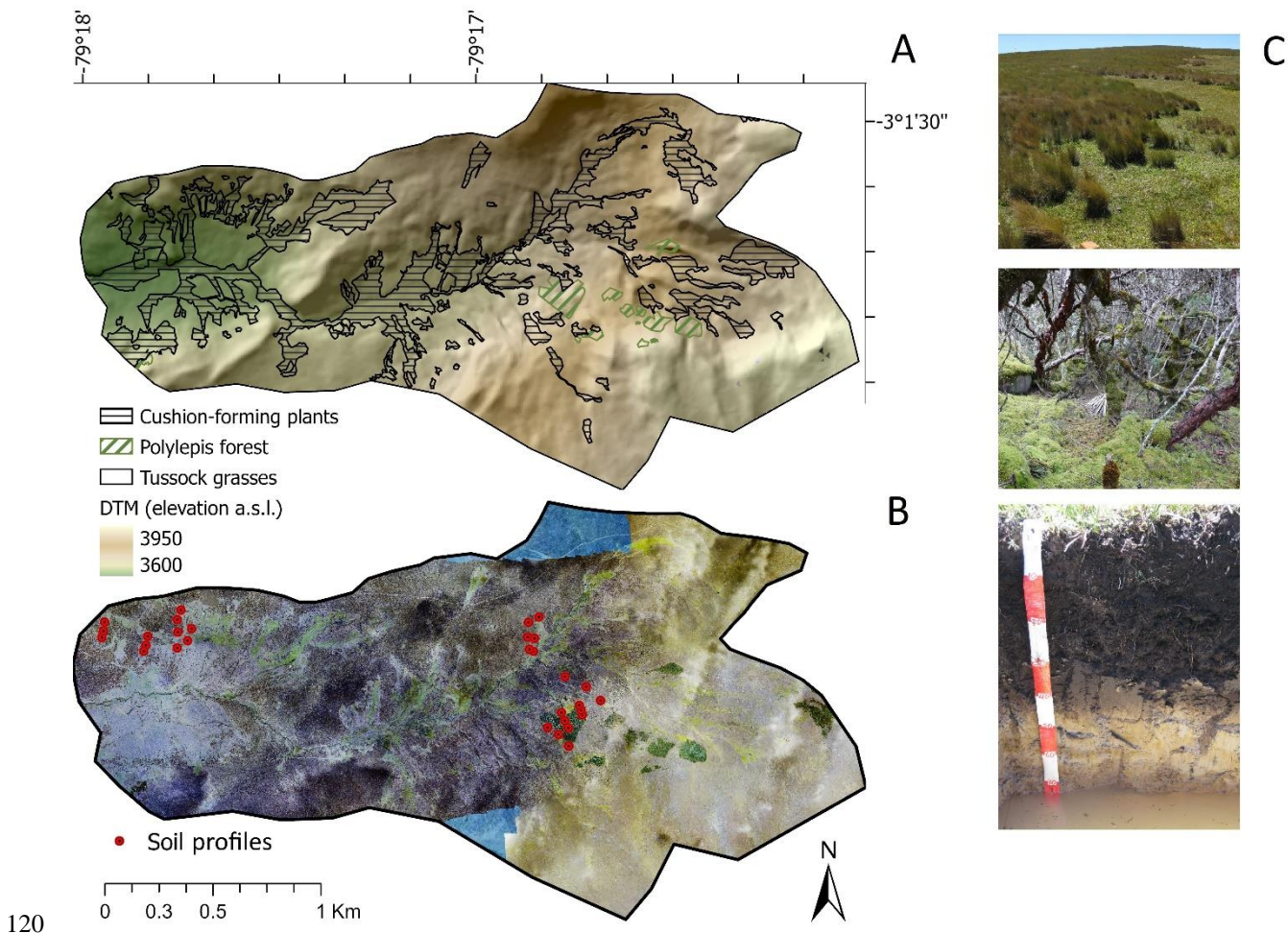
Figure 1: Overview of the three main vegetation assemblages in the high-altitude páramo ecosystem, with abundance of cushion-forming plants in topographic hollows and valley bottoms, tussock grasses along the hillsides and forest in poorly accessible areas

by humans. **(A) Representation of the topography with indication of the three vegetation types. (B) Composite of images taken by an uncrewed aerial vehicle with an indication of the location of the soil profiles. (C) Examples of the vegetation types, and one selected soil profile showing the importance of organic matter accumulation. The topographic and land use information was derived from aerial photographs taken by an uncrewed aerial vehicle using UAV-PPK-SfM techniques following Clapuyt et al. (2016) and Zhang et al. (2019).**

Summits and hillslopes have well-drained soils covered by bunch or tussock grasses, whereas toeslopes and valley bottoms are characterized by permanently waterlogged areas covered by hard cushion-forming plants. Forest patches are present on poorly accessible and steeper terrain in the upper part of the catchment. The vegetation pattern may result from local differences in microclimate and anthropogenic disturbances (Bader and Ruijten, 2008). Plant communities in the tussock-grass páramo consist mainly of bunch-grasses of the genera *Stipa* and *Calamagrostis* (Poaceae) (Jantz and Behling, 2012) and include Poaceae (*Paspalum*, *Cortaderia*), Hypericaceae (*Hypericum*), and Valerianaceae (*Valeriana*). Páramo wetlands are covered by cushion-forming plants, which comprise species of Plantaginaceae (*Plantago rigida*) and Cyperaceae (*Uncinia*) (Jantz and Behling, 2012; Coblentz and Keating, 2008). Woodlands contain small trees of 3 to 5 m height with the dominant species *Polylepis reticulata* (Fig. 1). Extensive grazing (by cattle and horses) had an impact on the landscape, but slowed down after 2010 when the land was declared a protected area. Traditional burning of grasslands is still practised in the wider region to remove old grass and allow nutritious, vigorous, new shoots to grow (White, 2013).

The nonallophanic Andosols developed on andesitic parent material from the Mio-Pliocene (Beate et al., 2001; Podwojewski and Poulenard, 2000; Buytaert et al., 2006). Soil formation started after the parent material was exposed following the retreat of glaciers during the late Pleistocene (Hansen et al., 2003). The young, postglacial soils experienced intense weathering with strong depletion of the Ca, Na, and K base cations throughout the soil depth (Molina et al., 2019). The presence of allophane is very limited, and soils are dominated by metal-humus complexes. The organic horizons have soil bulk densities as low as 0.28 g cm^{-3} and an organic carbon content up to 21%. Beyond the hillslope-scale topographic control on soil development, chemical and physical properties of soils differ by the soil weathering intensity and the type of vegetation. Soil depth (defined as depth to C horizon) varies across the vegetation communities, with average ($\pm$ 1 SD) soil depths of 65 $\pm$ 19 cm for tussock grasses, 61 $\pm$ 17 cm for forest, and 42 $\pm$ 6 cm for cushion plants. Using a chemical mass balance approach where mass losses or gains in soil are compared to parent material using Ti as a conservative element, Molina et al. (2019) showed that forest soils are strongly depleted in base cations (with total mass losses of 1440 kg.m^{-2}) followed by soils under tussock grasses (1210 kg.m^{-2}) and under cushion plants (1170 kg.m^{-2}). Soil acidity is enhanced by weathering, with a soil pH$_{H_2O}$ of 4.8 under forests, 5.0 under tussock grasses and 5.6 under cushion plants. Detailed information on the chemical weathering and soil development was reported earlier (Molina et al., 2019).

3. Materials and methods

3.1. Soil sampling strategy

Within the 4.2 km² study area, 33 sampling locations were selected: 9 under native polylepis forest, 9 under cushion-forming plants and 15 under the dominant vegetation cover, tussock grasses. An automatic weather station (Cancan Refugio, 3690 m a.s.l., ETAPA EP) records rainfall, air temperature and relative humidity at a height of 2.5 m above the ground. Soil pits were excavated to a depth of more than 15 cm below the soil weathering front, reaching depths of 57 to 120 cm. We sampled and described the soil profiles based on genetic horizons following the procedures of the World Reference Base for Soil Resources (Food and Agriculture Organization, 2006). Information on plant rooting depth was derived from field measurements during soil profile descriptions, and a distinction was made between the effective and the maximum rooting depth. The effective rooting depth corresponds to the zone where most of the roots grow in the upper horizons, and the maximum rooting depth to the deepest rooting depth observed in the C horizons. Soil and rock chemical analyses are described in Molina et al. (2019), and we re-used here the data on the exchangeable base cations and mass transfer coefficients (Table 1 and 3 in Molina et al., 2019) to assess the retention of rock-derived nutrients in the soil system. As the soil profiles have variable thicknesses, the bulk soil data were recalculated for multiple depth intervals of 20 cm each to facilitate inter-site comparison following the approach of Jobbágy and Jackson (2001).

3.2. Determination of hydrological and physical properties of the soil

We derived the volumetric soil moisture content, bulk density and water retention for a selection of 12 profiles: 3 under polylepis forest, 3 under cushion-forming plants, and 6 under tussock grasses. The A and C horizons of these profiles were sampled by taking undisturbed samples of 100 cm³ (in triplicate) in stainless steel rings and disturbed samples (700 g) in zip lock bags. Soil water retention curves were then determined from the experimental data on soil water retention for different matric potentials at the soil hydro-physical laboratory of PROMAS at the Universidad de Cuenca. Soil water retention at lower matric potentials (-100, -300, and -1500 kPa) was measured on saturated disturbed samples. Samples were mixed with water to a saturated soil paste which was then preserved in a closed container for 1 week. The soil paste was then placed in PVC rings on a pressure membrane in a container in which different pressures were applied, and samples are left for 7 days to equilibrate before measurement (Klute, 1986). At high matric potentials (0, -3, -6, -10, -24, and -46 kPa), the water retention was determined on undisturbed samples by the multi-step apparatus (van Dam et al., 1994). To estimate the gravimetric water content (g g^{-1}) for a given matric potential (kPa), the samples were weighted. At the end of the experiment, the samples were oven-dried at 80°C during 48 hours, and weighed again to obtain the soil bulk density (g cm^{-3}). This information was then used to convert the gravimetric water content (g g^{-1}) into volumetric water content (cm³ cm^{-3}). The soil water retention curves (12 sites × 2 horizons) were obtained by fitting a bimodal Van Genuchten model (Van Genuchten, 1980) through the measured soil water retention data following the approach described in Páez-Bimos et al. (2023).

Saturated hydraulic conductivity (K_s) of soils was measured in-situ on the A and C horizons of the 12 selected profiles using the inverse auger hole or so-called Porchet method (van Hoorn, 1979). We selected this method because of its extensive use in soils of páramo ecosystems (e.g. Buytaert et al., 2005; Marín et al., 2018, Páez-Bimos et al., 2022). The measurements were performed in fresh bore holes with 3 replicates per site. For further analyses, the average of the three measurements was taken.

3.3. Soil and rain water sampling

We sampled soil pore water using suction cup lysimeters (P80 ceramic, maximum pore size 1 µm; CeramTec AG, Marktredwitz, Germany). The 33 lysimeters were installed sub-horizontally at 50 cm depth, about 1 m upslope of the soil pits. At this depth, they collect soil solutions from the overlying A and AC horizons of the strongly weathered nonallophanic Andosols that are rich in organic matter as a result of biological activity including bioturbation and root growth (Molina et al., 2019). Rain water was sampled at the Cancan Refugio meteorological station where samples were collected with a plastic funnel connected to a 1 L bottle that was wrapped in aluminum paper and stored in a closed plastic bucket underground. The top of the funnel was covered with a 1 mm mesh, and a 20 µm nylon mesh was placed between the funnel and the hose. Lysimeters, tubes, and collection bottles were acid-washed and rinsed with deionized water before installation. The collection bottles (from dark glass) were closed with rubber stoppers, placed in plastic buckets with lids and buried in the ground approximately 2 m downslope of the lysimeters. Soil water was sampled biweekly from October 2012 to September 2013, with a few missing samples due to logistical constraints of working in a remote area. The initial 2-month equilibration period was estimated to be sufficient for the porous cups to equilibrate with the soil conditions following earlier work by Schwendenmann and Veldkamp (2005). Soil water was collected by applying a vacuum of 40 kPa to the collection bottles (Schwendenmann and Veldkamp, 2005; Kurniawan et al., 2018). During sample collection, the water collected was transferred to a clean high-density polyethylene bottle of 100 mL.

We measured the soil moisture potential in-situ using tensiometers (P80 ceramic, maximum pore size 1 µm; CeramTec AG, Marktredwitz, Germany). They were installed at the same depth as the lysimeters (50 cm) and at short distance (1 to 2 m). Soil water potential in the field was measured at the same time as soil water sampling, over the period October 2012 to September 2013. The data were converted into volumetric soil moisture values using measured soil water retention curves.

3.4. Soil water chemistry

Water samples were taken to the soil laboratory of the Faculty of Agricultural Sciences at the University of Cuenca (Ecuador) and frozen immediately. The frozen samples were transported by air to the University of Göttingen (Germany) where the chemical analyses were conducted. Analyses of total dissolved N (TDN), NH_4^+, NO_3^- and Cl^- were conducted using continuous-flow injection colorimetry (AA3; SEAL Analytical, Norderstedt, Germany); Dissolved organic C (DOC) was analyzed using a total organic carbon analyzer (TOC-Vwp; Shimadzu Europe, Duisburg, Germany). Analysis of base cations and total

dissolved Al, Fe, Mn S, P and Si was done using an inductively coupled plasma-atomic emission spectrometer (iCAP 6300; Thermo Fischer Scientific, Dreieich, Germany). For details and detection limits we refer to Kurniawan et al. (2018). We reported all solute concentrations in $\mu mol_c\ L^{-1}$ (molar concentration multiplied by the equivalent charge of the solute). A partial cation-anion charge balance of the major solutes (i.e., those with concentrations $> 2\ \mu mol_c\ L^{-1}$) was performed, considering all pore water samples of a given vegetation type following the methods described in Kurniawan et al. (2018). The contribution of bicarbonates (HCO_3^-) and organic acids ($RCOO^-$) were estimated by subtracting the total anion charge from the total cation charge, whereby the charge contributions of the total Al were assumed to be 3^+. Solute concentrations that exhibited very low levels (i.e., total Fe, Mn, and P), and thus had minimal charge contribution were excluded from the calculations (following the method used by Hedin et al., 2003).

Given the lack of Cl-bearing minerals in the parent material, the pore water Cl concentrations were used to estimate evapotranspiration rates and soil water fluxes. We used the approach of White et al. (2009) and Buss et al. (2017) to estimate soil hydrological fluxes from the chloride concentrations in rain and soil water. Assuming 1D vertical flow, the fluid flux density was calculated as the net difference between annual precipitation and evapotranspiration fluxes, and equal to the product of precipitation and the ratio of volume-weighted Cl concentration in precipitation to that in soil pore water (Buss et al., 2017). The average infiltration rate was then calculated by dividing the fluid flux density by the product of the average porosity and saturation, and the average fluid residence time by taking the ratio of the profile thickness and the infiltration rate. To evaluate the role of vegetation uptake on plant nutrient concentrations in the soil solution, we analyzed nutrient/Cl ratios. Chloride is not an essential nutrient and not actively assimilated by the vegetation (Boxman et al., 2008) and changes in the soil water Cl concentrations are thus mainly caused by difference in soil water balance if we assume that the Cl input through weathering and deposition does not vary between sites. An increase in nutrient/Cl ratios indicates an enrichment of the nutrient relative to Cl, and a decrease a removal of the nutrient relative to Cl.

3.5. Statistical analyses

We used linear mixed-effects (LME) models (Crawley, 2009) to test whether soil development, soil hydrology and nutrient availability were different in soils covered by cushion-forming plants, tussock grasses and polylepis forest. The model used the vegetation type as the fixed effect, and the spatial replication (experimental sites) and monitoring time (biweekly or monthly measurements) as random effects. In total, 360 samples from 31 experimental sites were used for the statistical analysis, as we excluded the data from two forested sites (FR1 Middle, FR3 Upper) where exceptionally high solute concentrations were measured, larger than two standard deviations above the average. Differences between vegetation types (fixed effects) were assessed based on analysis of variance at $p \leq 0.05$. Correlation between explanatory variables was tested with Spearman's rank correlation statistics, and we reported the strength and type of association by the Spearman's rho and p-values. The R software version 3.1.2 (R Development Core Team, 2014) was used to perform all the statistical analyses.

4. RESULTS

4.1. Variations in soil and vegetation rooting depth

The young volcanic soils were generally thin and the depth to the C horizon ranged from 27 to 100 cm. Soils under cushion-forming plants were thinner (42 ± 6 cm) than under forests (61 ± 17 cm) and tussock grasses (65 ± 19 cm, Table 1 in Molina
255 et al., 2019). The effective rooting depth of the vegetation was lower under cushion-forming plants than under forests or tussock grasses with depths of 33 ± 4 cm under cushion plants, and about 10 cm more in forests (44 ± 6 cm), and tussock grasses (41 ± 8 cm, Fig. 2). The maximum rooting depth followed the same pattern with 51 ± 8 cm under cushions, 82 ± 16 cm under forest, and 75 ± 17 cm under tussock grasses (Table S1). The root systems of trees and tussock grasses allow the plants to acquire water and nutrients at significantly greater depths than cushion-forming plants. Some of the deepest roots
260 extended to more than 1 m in well-drained soils developed under forest or tussock grasses. Effective and maximum root depths were positively associated to the soil depth, illustrating the strong link between soil development, plant growth and root development (Spearman's rho = 0.78 and 0.75 resp., p-value < 0.01, n = 31).
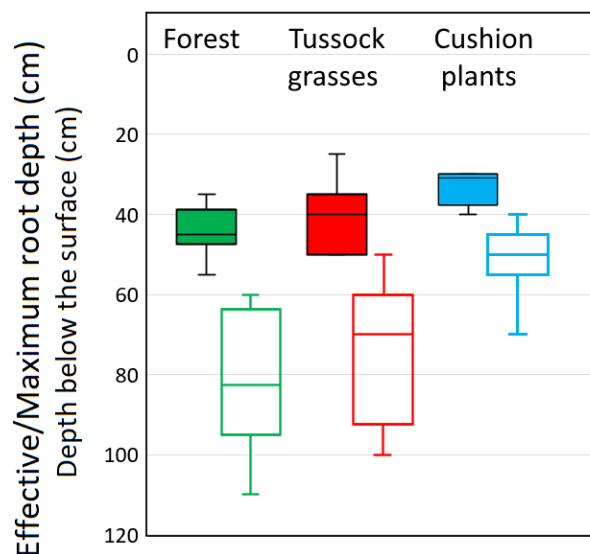
265 **Figure 2: Depth-distribution of root development in forests (n=9, green), under tussock grasses (n=15, red) and cushion-forming plants (n=9, blue). The effective rooting depth contains > 90% of the root biomass and corresponds to the maximum depth at which vegetation effectively uses plant-available water. The maximum rooting depth refers to the deepest rooting depth observed in the C horizons.**

4.2. Nutrient distribution in the soil profile

270 All soils experienced intense chemical weathering with significant elemental depletion throughout the soil profile (Fig. 3). Total weight losses by chemical weathering for the 30 profiles ranged between 793 and 1610 kg.m^{-2}, with a mean value of

1240 ± 210 kg.m^{-2} (Table 3 in Molina et al., 2019). Depletion profiles did not show a clear trend in base cation loss with depth and had a rather uniform depletion of Ca, Na, K, and Mg throughout all horizons. The chemical mass losses were significantly different between vegetation types: soils covered by cushion-forming plants had the lowest chemical mass losses. Being

275 significantly less depleted in Ca, Na, and K, their remaining stock of rock-derived nutrients was higher than in soils under forests and tussock grasses. The lithogenic elements that were biotically cycled by plants - Ca, K and Mg - had the highest concentrations of mean exchangeable cations in the upper 20 cm of the profiles, and then decreased with depth up to 60 cm (Fig. 3). This pattern was observed under all vegetation types and we inferred that they were being biotically pumped to the surface horizons. The lowest concentrations of exchangeable and total Ca and K were measured between 60 and 80 cm depth

280 which corresponds to the average maximum rooting depth. The exchangeable Ca and Mg concentrations varied between vegetation types (Table 1). Soils under cushion plants had 82% higher exchangeable Ca and ~72 to 62 % higher exchangeable Mg concentrations than under forests or tussock grasses (Table 2). In contrast to the Ca, K and Mg soil cations, the Na cation concentration increased with soil depth under cushion plants although the absolute depth-variations were small. Similar to the other biotically cycled elements, the exchangeable Na concentrations were significantly higher under cushion-forming plants.

285
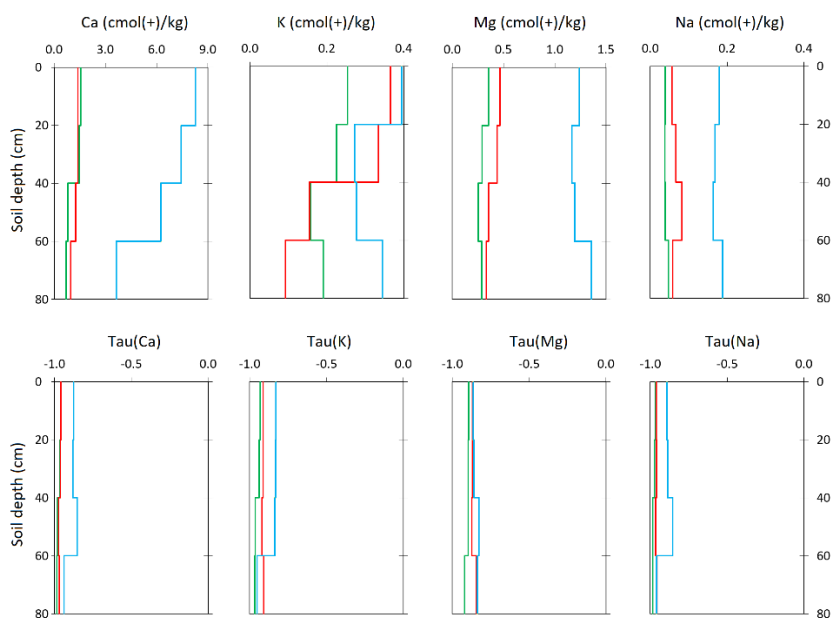
Figure 3: Depth-variation of the mean exchangeable Ca, K, Mg, and Na concentrations, and their mean elemental mass transfer coefficients in soils under forests (n=7, green line), tussock grasses (n=15, red line) and cushion-forming plants (n=9, blue line).

Table 1. Summary of the linear mixed-effect model, with indication of the significance level of the fixed effects (vegetation type). The mean annual concentrations of the major elements and pH per vegetation type are given in Table 2.

Nutrient/Element in soil solution	Cushion plants vs tussock grasses	Cushion plants vs forest	Tussock grasses vs forest
Calcium (Ca)	< 0.001	< 0.001	0.991
Potassium (K)	0.827	< 0.050	< 0.010
Magnesium (Mg)	< 0.001	< 0.010	0.845
Sodium (Na)	< 0.001	< 0.001	0.906
Total silica (Si)	< 0.001	< 0.001	0.740
Total phosphorus (P)	0.801	0.596	0.774
Total aluminum (Al)	< 0.010	< 0.001	< 0.010
Total Iron (Fe)	< 0.010	< 0.001	< 0.010
pH	< 0.001	< 0.001	< 0.001

Table 2: Mean annual concentration (± 1 SD) of the major elements and pH in the soil solution under forest, tussock grasses and cushion-forming plants measured monthly from October 2012 till September 2013.

	Ca	K	Mg	Na	Si	P	Cl	S	Al	Fe	pH
	μM (mean ± 1 SD)										
Forest	28±18	38±28	14±7	69±50	18±22	0.2±0.1	20±4	11±4	13±8	1±0	5.7±0.6
Tussock grasses	19±7	11±8	9±3	58±29	39±38	0.3±0.3	15±10	4±1	2±1	1±2	6.5±0.2
Cushion plants	82±36	17±10	24±10	181±81	291±135	0.2±0.1	20±9	4±2	1±1	3±3	7.1±0.2

4.3. Soil hydrological properties

4.3.1. Spatiotemporal variation in soil moisture content

The annual rainfall measured at Cancan Refugio was 546 mm, about 40 % less than the mean annual rainfall in this region (ETAPA EP). The monitoring period (October 2012 to September 2013) coincided with a severe drought and 2012 and 2013 were amongst the driest years on record. Most of the rain (71%) fell during the wet season (i.e., between November 2012 and May 2013, Fig. 4) although April was unusually dry. The soil moisture pattern followed the overall rainfall seasonality with highest volumetric soil water contents (SWC, in $cm^3.cm^{-3}$) in the wet season between November and June, and the lowest values between July and October. Despite the unusually low precipitation amount registered over the monitoring period, the volumetric soil water content remained high in all 33 soil profiles (i.e. above 0.40 $cm^3.cm^{-3}$, Table S1) and rather constant over the wet season and it declined only gradually during the dry months. The temporal variation in soil moisture content was similar for all vegetation types, with SWC values below the mean annual SWC over the dry months. Clear differences were observed in the absolute soil moisture content between vegetation types: over the monitoring period, the volumetric soil water content under cushion-forming plants was, on average, 7% higher than under tussock grasses and 16% higher than in forests

310 (Fig. 4). Forests experienced the lowest soil water availability, with SWC approaching the wilting point during the driest month.
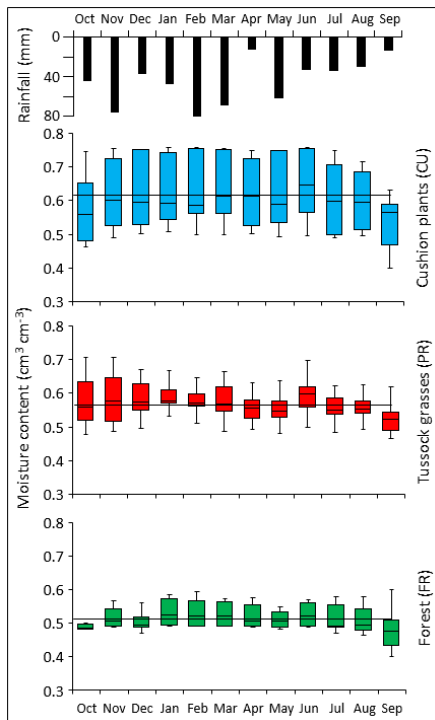
Figure 4: Mean monthly rainfall (mm) and mean monthly soil moisture content (cm³.cm⁻³) in soils under cushion-forming plants
315 **(mean annual SWC ± 1 SD: 0.61 ± 0.08 cm³.cm⁻³), tussock grasses (0.57 ± 0.04 cm³.cm⁻³) and forest (0.51 ± 0.03 cm³.cm⁻³).**

4.3.2. Saturated hydraulic conductivity and water residence time

The saturated hydraulic conductivity (K_s) differed between vegetation types and between A and C horizons. The K_s was highest in the A horizons of forest soils, followed by cushion-forming plants and tussock grasses (Fig. 5, Table S2). The K_s of the C

320 horizons was highly variable between vegetation types, with the highest values under forests and the lowest under cushion-forming plants. The saturated hydraulic conductivity was close to 0 mm.h⁻¹ in the C horizons under cushion-forming plants, indicative of the presence of an impermeable layer at the contact between soil and weathered parent material. Calculated water residence time in the soils was overall high (i.e., above 200 days). Forest and tussock grasses had similar residence times of about 202 and 203 days, while soils covered by cushion-forming plants showed a longer water residence time of 231 days

325 (Fig. 5). This points to the fact that cushion-forming plants were abundant in soils that were prone to undergo waterlogging or saturation during the rainy season, even in unusually dry years (Table S3). Given that the monitoring period was unusually

dry, the differences in water residence time can be higher during normal rainfall years, and further monitoring is necessary to study the potential effect of drought on water residence time.
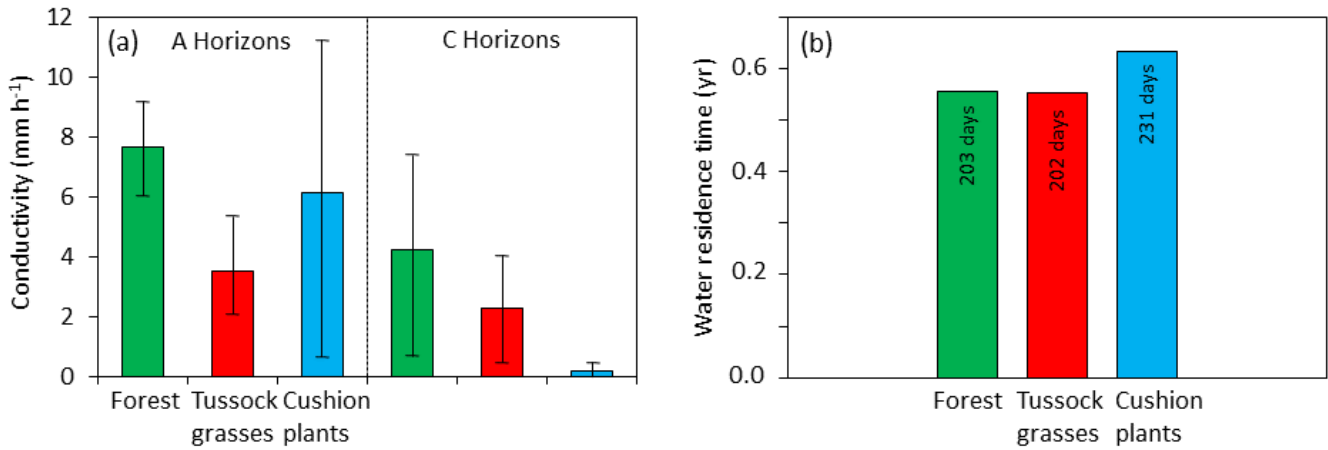
330

Figure 5: Mean saturated hydraulic conductivity (mm h⁻¹) and mean water residence time (yr) under forest, tussock grasses and cushion-forming plants for period between October 2012 and September 2013.

4.4. Soil solute chemistry

335   The mean pH in water of the soil solutions differed between vegetation types with acidic conditions under forests (5.7 ± 0.6) and tussock grasses (6.5 ± 0.2), and near neutral conditions under cushion-forming plants (7.1 ± 0.2, Table S4). The total ionic charge of the soil solution under cushion-forming plants was about twice the concentration measured under forests and three times the concentration under tussock grasses (Table 2). The major ions contributing charge in the soil solutions were rather similar between vegetation types, with Na > Ca > >Mg or K cations, and HCO_3^- >> Cl anions, although NO_3^- and K

340   contributions were higher under forests than under cushion-forming plants and tussock grasses (Fig. S1). On annual basis, the concentrations of solute Ca, Mg, Na and Si were higher under cushion-forming plants, whereas the solute K concentration was higher under forest (Table 2). Solute Al showed the highest concentrations under forest and lowest concentrations under cushion plants, whereas solute Fe showed the opposite pattern (Fig. S2). Dissolved P concentrations were close to the detection limit in the soil solution and we did not detect significant differences between vegetation types. When accounting for the

345   difference in soil water balance between vegetation types, the Ca/Cl and Mg/Cl ratios under cushion plants were at least twice as high as under forests and tussock grasses (Fig. 6). Over one hydrological year, we noticed only minor temporal variation in Ca, Mg, Na and Si solute concentrations under forest and tussock grasses, whereas there existed large variation in these concentrations under cushion plants (Fig. 7). Seasonal variation in nutrient/Cl ratios was stronger, particularly under cushion plants, where it showed clear variations throughout the year with peaks during the rainy season (Fig. S3). Solute K

350 concentrations behaved differently than the other cations, with forests having the highest K/Cl ratio and peaks in K/Cl ratio during the rainy season. Unlike other mineral solutes, temporal variations of solute P were similar in all vegetation types.
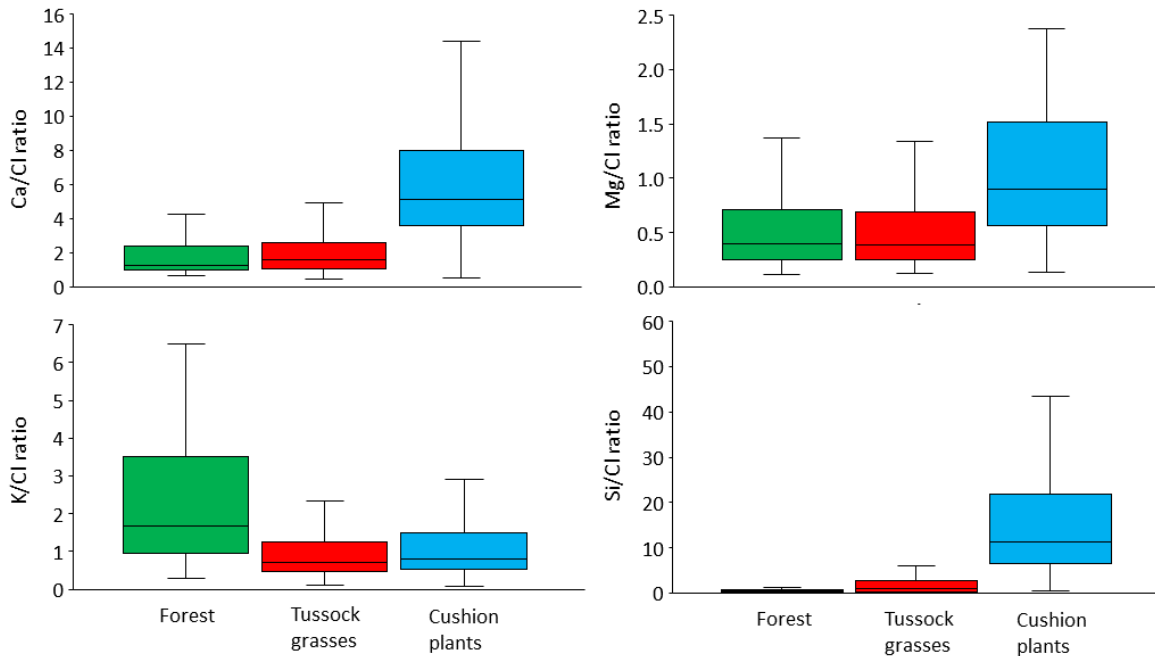
355 **Figure 6: Ratio of Ca, Mg and K nutrients to Chloride in the soil solution of forests (n=7), tussock grasses (n=15) and cushion plants (n=9). An increase in the ratio indicates an enrichment of the nutrient relative to Cl, and a decrease a removal of the nutrient compared to Cl.**

360 **4.5. Relationship between soil moisture and solute concentrations**

Soil solute concentrations varied between vegetation types and with soil moisture levels, with the exception of solute P concentrations that were consistently low at all soil moisture levels and under all vegetation types (Fig. 8). Cushion plants colonized the wettest zones where the highest Ca, Mg, Na and Si solute concentrations were measured. Tussock grasses were dominant in soils with intermediate soil moisture contents and were characterized by the lowest soil solute concentrations 365 (except Si). Forest soils had the lowest soil moisture contents over the hydrological year, and they had particularly high solute K and low Si concentrations. For all vegetation types combined, the volumetric soil water content was positively related (r ≥ 0.6, n = 36) to the soil solute Ca, Na, and Si concentrations, and negatively related (r = -0.6, n = 36) to the soil solute K concentrations. Soil solute Mg and P concentrations were independent of the soil moisture content.
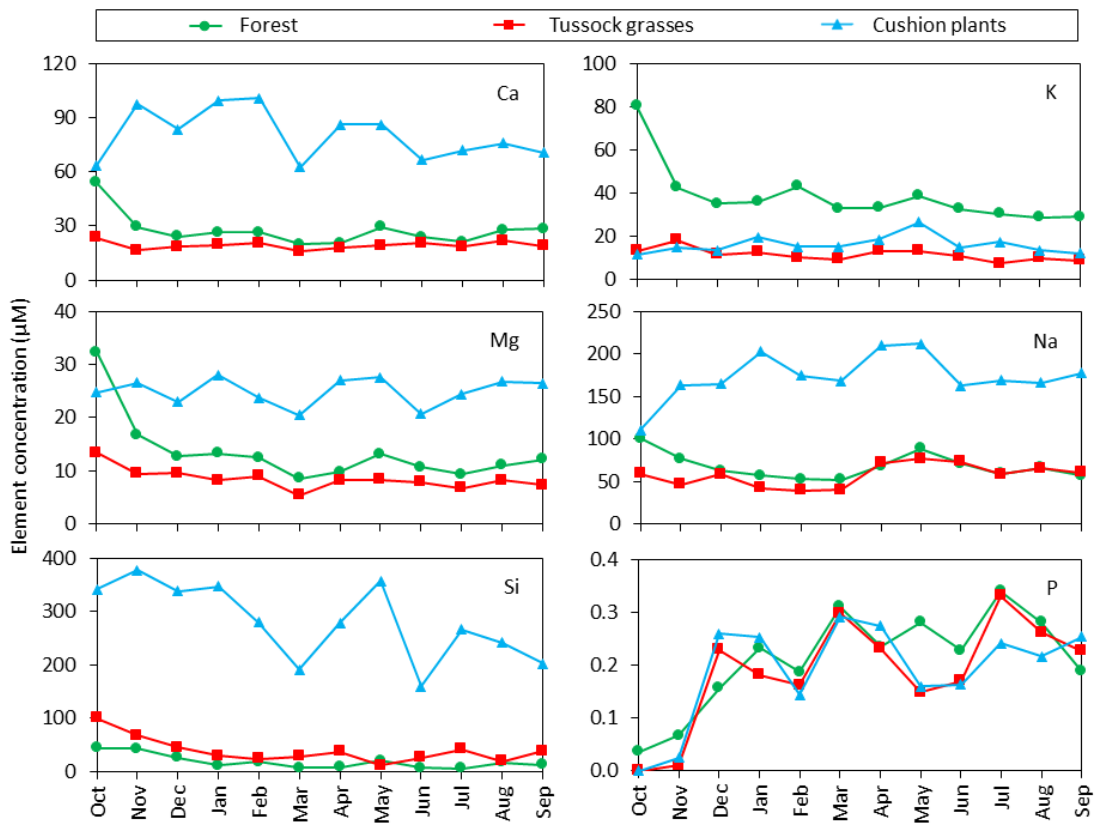
370

Figure 7: Temporal variation in soil solute concentrations under forest (n=7), tussock grasses (n=15) and cushion plants (n=9). The mean monthly values for the period October 2012 till September 2013 are plotted in the graphs. Even after a 2-month equilibration period, we cannot entirely exclude that the first cation concentration measurements under forest (October 2012) are higher-than-expected due to incomplete stabilization of the lysimeters after installation (e.g. preferential flow because of lysimeter insertion).

375
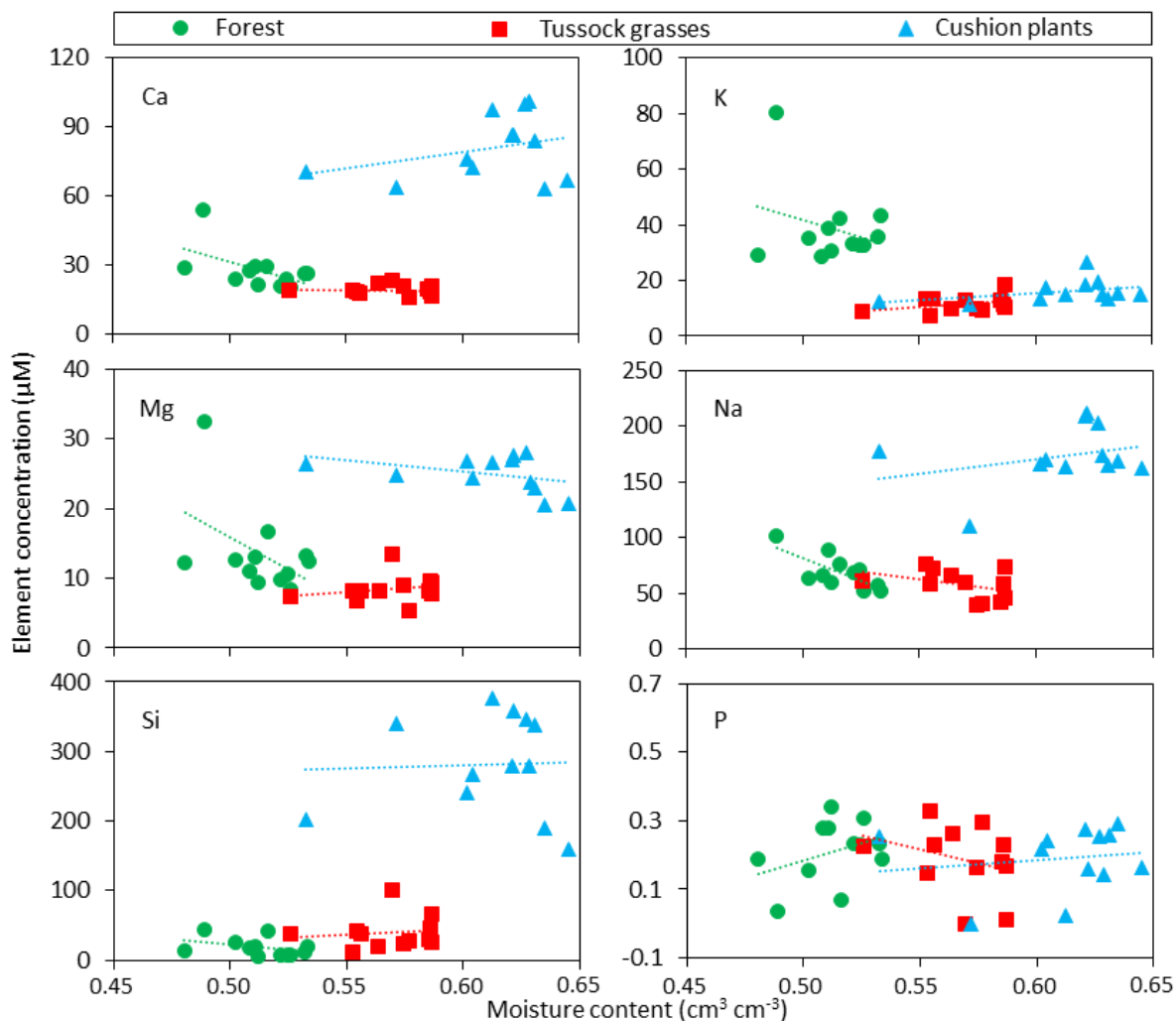
Figure 8: Relation between soil solute concentrations and soil moisture contents under forest, tussock grasses and cushion plants.

5. DISCUSSION

5.1. Soil moisture regulation by plant rooting depth

380   Plants employ different mechanisms to acquire water and mineral nutrients that are required for their adequate growth. Adaptation mechanisms include changes in the rooting depth so that the plants can access new sources of water and nutrients from within the weathering mantle (Schenk and Jackson, 2002). Plant rooting depth plays a key role in regulating soil-water processes (Fan et al., 2017). In the High Andes, vegetation patterns covary with slope morphology, and plant rooting depth

385   varies with soil drainage, topographic position, and soil development. Our results reveal strong differences in plant rooting depth at the landscape scale, that are associated with soil moisture and vegetation patterns.

5.1.1. Soil moisture-regulated rooting depth under cushion plants

Cushion plants are prevalent in topographic concavities and hollows where soils are seasonally waterlogged or saturated. Although dense vegetation cover facilitates rapid soil water infiltration in the organic-rich A horizons, the water percolation to deeper subsoil is limited by very low saturated hydraulic conductivity of the C horizon. In the poorly conductive subsoil, water stagnation was evidenced by long water residence times, and reducing conditions occurred as shown by high levels of dissolved Fe in soil solutes. The soil solutes in sites with low water flow rates tend to approach chemical equilibrium following Maher (2011), and, hence, they limit the potential for in situ chemical weathering and soil thickening. Cushion plants are favored in these environments where the plant rooting depth is often limited by prolonged soil saturation and anoxia during the wet season. At the same time, the colonisation by cushion-forming plants leads to a positive feedback as the shallow but coarse rooting system of cushion plants (with root diameter > 2mm, Páez-Bimos et al., 2022) does not penetrate deeper soil horizons where roots could create pathways for future subsurface flow.

5.1.2. Soil moisture-regulated rooting depth under forests and tussock grasses

Forest and tussock grasses typically colonized linear and convex slopes that were characterized by soil water infiltration rates above 2 mm.h^{-1} in A and C horizons. In these well-drained soils, the rooting depth followed infiltration depth and deep roots were found at more than 1 m depth. Deep soil water infiltration enabled plant root systems to develop and mine water at depth. As shown for temperate (Rempe and Dietrich, 2018) and humid (Jobbágy and Jackson, 2007) environments, deep root systems can gradually deplete soil moisture storage due to higher transpiration losses during the dry season. The difference in soil moisture content between forests and tussock grasses was not related to the effective root depth, but likely to be related to plant water status, i.e. the balance between water uptake by roots and water loss through transpiration from leaves. Compared to forests, the canopy interception and evapotranspiration was lower under tussock grasses (Páez-Bimos et al., 2023), which makes them more tolerant to water stress. Rada et al. (2019) showed for the Venezuelan páramos that grasses were more tolerant to water stress than shrubs or trees at moments when soil water availability was limited due to high temperatures and evaporative demand.

5.2. Spatiotemporal variations in soil solution chemistry

In our study area, the highly weathered nonallophanic Andosols contain low stocks of mineral nutrients, suggesting a low supply of rock-derived nutrients relative to the demand by the ecosystem. Under these conditions of nutrient-limited soils, biological processes play an important role in controlling soil solution chemistry: soil solute chemistry revealed patterns in plant available nutrients that were not mimicking the distribution of total rock-derived nutrients nor the exchangeable nutrient

pool, but clearly resulted from strong biocycling of cations and removal of nutrients from the soil by plant uptake or deep leaching.

5.2.1. Soil solute dynamics under cushion plants

Soil solutes under cushion-forming plants had the highest concentrations in Ca, Mg, Na and dissolved Si, as a result of low
420 plant root uptake, and low saturated conductivity at depth. As a result of low subsoil conductivity, soils became waterlogged during the wet season as shown by long water residence times and reduced conditions. Consequently, soils under cushion plants had the lowest soil weathering intensities and neutral soil pH_{H_2O}. The plant-generated effects on soil chemistry were visible in the distribution of exchangeable Ca, Mg, and Na in the top 80 cm of the soil. Exchangeable Ca and Mg were enriched in the upper soil horizon, indicating that these cations were highly biocycled. Contrary to expected (Jobbagy and Jackson,
425 2004; White et al., 2012), sodium was slightly enriched in the upper horizons which can be indicative of evaporation concentration of Na or biocycling of Na by cushion-forming plants. Pools of available Ca and Mg are influenced by plant biocycling, but nutrient/Cl ratios were disproportionally large in the waterlogged soils underlying the cushion plants. On an annual basis, the Ca/Cl and Mg/Cl ratios in soil solutions under cushion-forming plants were 3.1 and 2.3 times higher than under forest and 3.2 and 2.5 times higher than under tussock grasses. Differences in Si/Cl ratios were even larger between
430 vegetation types, with Si/Cl ratios under cushion-forming plants being 14.0 times higher than under forest and 6.2 times higher than under tussock grasses. Solute K and P showed different patterns, possibly due to the importance of near-surface supply of those two cations and minimal deep leaching under cushion-forming plants.

5.2.2. Soil solute dynamics under forests and tussock grasses

435 The water movement through deep weathering profiles, deep roots, and plant biocycling exert strong controls on solute concentrations in forest and grassland soils. The soil exchangeable Ca, Mg, and K showed the highest concentrations in the top 20 cm of soil, indicating that these cations were strongly cycled and retained by plants. Biocyling of potassium can be particularly important in forest because of the relatively high nutrient demand of trees such as *Polylepis reticulata* for their physiological activities. Potassium is typically found in highest concentrations in plant tissues (Jobbagy and Jackson, 2004)
440 and plays a major role in the osmotic balance and photosynthesis (Tripler et al., 2006).

Under forest, the soil pore waters contained remarkably high K concentrations and K/Cl ratios, given their relatively low K availability in the soil exchangeable phase and bulk soil (compared to cushion plants and tussock grasses, Fig. 3). Forest soils experienced the driest soil water conditions throughout the hydrological year, and tree roots effectively pump water and nutrients from deeper horizons than grasses and cushion plants. Deep biological pumping of K resulted in elevated near-surface
445 concentrations of K in forest topsoil that were 2 to 3 times higher than under tussock grasses and cushion plants.

Other soil solutes (Ca, Mg, Na and Si) had similar concentrations under forest as under tussock grasses. In these well-drained soils, the pool of plant available nutrients (e.g., Ca and Mg) are largely controlled by water percolation and leaching losses. The importance of such processes in soil nutrient depletion in volcanic soils was shown earlier by e.g., Chadwick et al. (2003). The remaining soil exchangeable Ca and Mg was strongly concentrated in the topsoil horizons, and the result of strong biogenic

450 control on Ca and Mg distributions. Calcium is a vital structural component of plant tissues and important for cell synthesis (McLaughlin and Wimmer, 1999), and Mg is a critical constituent of chlorophyll and many cellular enzymes and, therefore, important for photosynthesis (Shaul, 2002). In contrast to the soil exchangeable Ca and Mg distributions, Na was more concentrated at depth indicating that it was not retained in the topsoil but leached to deeper horizons. Sodium is not an essential plant nutrient and tends to be excluded by plant roots, typically resulting in greater Na concentrations in deeper soil horizons

455 (Jobbagy and Jackson, 2001; White et al., 2012). Under tussock grasses, there was a slight increase in exchangeable Na in the deeper horizons while there was no change in exchangeable Na concentrations under forest. Deep leaching of Na is important under forest and tussock grasses, and resulted in low Na concentrations in soil solutions. This is further confirmed by the fact that soil solute Na concentrations decreased with increasing soil moisture, i.e., during the wetter months when higher leaching losses occurred.

460 Amongst the nutrients derived from lithogenic sources, P and K are often limiting plant development and use to be strongly biocycled (Jobbagy and Jackson, 2001). The very low soil solute P concentrations (i.e. below 1 µM) manifest a high vegetation demand of P and low solubility. The highly weathered Andosols are nonallophanic and contain high levels of organometallic (Al-humus) complexes (Molina et al., 2019). Previous work in nonallophanic Andosols showed that P retention is high (i.e., > 95%) in topsoil and subsoil (Poulenard et al., 2003; Buytaert et al., 2006), which strongly limits the amount of soluble P in the

465 soil solution, and reduces plant P uptake (Bol et al., 2016). The low soil solute P concentrations can be attributed to the strong P sorption on the Al-humus complexes. Furthermore, the formation of metal-humus complexes in nonallophanic Andosols increases the P fixing capacity by protecting it from microbial and enzymatic decomposition (Delfim et al., 2018; Borie et al., 2019), and no differences in P availability or solute concentrations were observed between vegetation types (Fig. S2).

6. CONCLUSION

470 The páramo landscape in the High Andes forms a vegetation mosaic of bunch-grasses, cushion-forming plants and forest patches. This study on soil-water-vegetation interactions evaluated the association between vegetation, soil hydrology and mineral nutrient availability at the landscape scale. In the highly nutrient-depleted nonallophanic Andosols, the plant rooting depth varies with drainage and soil moisture conditions. Topographic depressions that are seasonally waterlogged mainly comprise shallow soils, and shallow-rooted plants such as cushion-forming vegetation. In comparison, hillslopes contain

475 deeper and better drained weathering profiles, and are colonised by bunch grasses and trees whose rooting systems extend to more than 100 cm depth. The soil-depth variations that are observed at the landscape scale indicate that lateral redistribution of soil particles along slopes is likely to be slow in such preserved paramo ecosystems. The type of vegetation is a relevant

indicator of the availability of rock-derived nutrients in the soil solutions. Soils under cushion-forming plants showed solute concentrations of Ca, Mg and Na of about 3 times higher than forest and tussock grasses, and solute concentrations of Si were 16 times higher than forest and 6 times higher than tussock grasses where intense cation leaching and plant nutrient retention depressed the lithogenic solute concentrations. Potassium clearly showed different behaviour than the before-mentioned cations: while the total K stock and exchangeable K in the soil were lowest under forests, their soil solute K concentrations and K/Cl ratios were 2 to 3 times higher than under cushion-forming plants or tussock grasses. The soil solute chemistry revealed patterns in plant available nutrients that are not solely mimicking the distribution of total rock-derived nutrients or the exchangeable nutrient pool, but that clearly resulted from strong biocycling of cations and removal of nutrients from the soil by plant uptake or deep leaching.

Our findings have important implications for future management of Andean paramo ecosystems where vegetation type distributions are dynamically changing as a result of warming temperatures and land use policies with regard to livestock grazing, soil tillage and use of fire. Our results put forward that vegetation communities are related to soil chemical weathering extent, hydro-physical properties and hydrochemistry of soil pore waters. As such, changes in vegetation distributions will not only lead to changes in soil hydrology and solute geochemistry but may also lead on to complex changes in weathering rates and solute export downstream with effects on nutrient concentrations and, hence, aquatic ecology of Andean rivers and high-mountain lakes. Our results ask for further evaluations of vegetation-related soil water and solute fluxes, including coupling of soil moisture and solute chemistry with water fluxes and upscaling of hydrochemistry from soil profile to ecosystem scale.

Data availability

All data used in this paper are archived and will be publicly available in the UCLouvain DataVerse upon final publication of the paper.

Supplement

The supplement related to this article contains four supplementary figures and four supplementary tables. The pdf containing the supplements is provided with the submission, and will be available online upon final publication of the paper.

Author contributions

Conceptualization: AM, EV, VV: experimental design: AM, VV; data collection: AM, SZ; data validation: AM, OC, MC, VV; interpretation and analyses: AM, VV, OC, EV; funding acquisition: AM, VV; project administration: AM, EV; writing – original draft: AM, VV; writing – review and editing: all authors.

Competing interests

At least one of the (co-)authors is a member of the editorial board of Biogeosciences.

Acknowledgements

510 We thank Marco Ramirez and Oscar Morales for assistance and support during the field campaigns, and are grateful for the help of several undergraduate students (Juan Barahona, Tanya Contreras and René Fernández) of the Universidad de Cuenca. Eduardo Tacuri and Mateo López realised the UAV flights over the study area, and provided the very high resolution topography and imagery. We acknowledge Sandra Barros and Javier Fernández de Cordoba of ETAPA EP (Empresa Pública Municipal de Telecomunicaciones, Agua Potable, Alcantarillado y Saneamiento de Cuenca) for continued support of our

515 research activities in the High Andean headwater basins, and want to express our appreciation to Felipe Cisneros of PROMAS (Programa para el Manejo del Agua y del Suelo, Universidad de Cuenca) for continued support.

Financial support

Armando Molina received a Georg Forster Fellowship for Postdoctoral Researchers (3.2-ECU/1138588 STP) from the Alexander von Humboldt Foundation, and a Prometeo grant from the Secretaría de Educación Superior, Ciencia, Tecnología

520 e Innovación from the Ecuadorian government. Additional support was provided by the research cooperation projects "Strengthening the scientific and technological capacities to implement spatially integrated land and water management schemes adapted to local socio-economic, cultural and physical settings" (CUD PIC-09 Ecuador) and "Linking Global Change with Soil and Water Conservation in the High Andes" (ARES PRD-17 ParamoSus) funded by the Académie de Recherche et d'Enseignement Supérieur de la Fédération Wallonie-Bruxelles (ARES) of Belgium.

525 **References**

Amundson, R., Richter, D. D., Humphreys, G. S., Jobbágy, E. G., and Gaillardet, J.: Coupling between Biota and Earth Materials in the Critical Zone, Elements, 3, 327-332, https://doi.org/10.2113/gselements.3.5.327, 2007.

Amundson, R.: An Introduction to the Biogeochemistry of Soils., Cambridge, UK, Cambridge University Press, ISBN: 978-1-108-83126-0, 2021.

530 Bader, M.Y. and Ruijten, J.J.A.: A topography-based model of forest cover at the alpine tree line in the tropical Andes. Journal of Biogeography, 35: 711-723, https://doi.org/10.1111/j.1365-2699.2007.01818.x, 2008.

Beate, B., Monzier, M., Spikings, R., Cotton, J., Silva, J., Bourdon, E., and Eissen, J . P.: Mio-Pliocene adakite generation related to flat subduction in southern Ecuador: The Quimsacocha volcanic center, Earth. Planet. Sc. Lett., 192, 561-570, https://doi.org/10.1016/S0012-821X(01)00466-6, 2001.

535   Bol, R., Julich, D., Brödlin, D., Siemens, J., Kaiser, K., Dip- pold, M. A., Spielvogel, S., Zilla, T., Mewes, D., von Blanck-enburg, F., Puhlmann, H., Holzmann, S., Weiler, M., Amelung, W., Lang, F., Kuzyakov, Y., Feger, K. H., Gottselig, N., Klumpp, E., Missong, A., Winkelmann, C., Uhlig, D., Sohrt, J., von Wilpert, K., Wu, B., and Hagedorn, F.: Dissolved and colloidal phosphorus fluxes in forest ecosystems – an almost blind spot in ecosystem research, J. Plant Nutr. Soil Sc., 179, 425–438, https://doi.org/10.1002/jpln.201600079, 2016.

540   Borie, F., Aguilera, P., Castillo, C., Valentine, A., Seguel, A., Barea, J. M., and Cornejo, P.: Revisiting the nature of phosphorus pools in Chilean volcanic soils as a basis for arbuscular mycorrhizal management in plant P acquisition, Journal of Soil Science and Plant Nutrition, 19, 390-401, https://doi.org/10.1007/s42729-019-00041-y, 2019.

Boxman, A. W., Peters, R. C., and Roelofs, J. G.: Long term changes in atmospheric N and S throughfall deposition and effects on soil solution chemistry in a Scots pine forest in the Netherlands, Environ. Pollut., 156, 1252-1259,

545   https://doi:10.1016/j.envpol.2008.03.017, 2008.

Brantley, S. L. and White, A. F.: Approaches to modeling weathered regolith, Reviews in Mineralogy and Geochemistry., 70, 435-484, https://doi.org/10.2138/rmg.2009.70.10, 2009.

Brantley, S. L., Eissenstat, D. M., Marshall, J. A., Godsey, S. E., Balogh-Brunstad, Z., Karwan, D. L., Papuga, S. A., Roering, J., Dawson, T. E., Evaristo, J., Chadwick, O., McDonnell, J. J., and Weathers, K. C.: Reviews and syntheses: On the roles

550   trees play in building and plumbing the critical zone, Biogeosciences, 14, 5115–5142, https://doi.org/10.5194/bg-14-5115-2017, 2017.

Buss, H. L., Chapela Lara, M., Moore, O. W., Kurtz, A. C., Schulz, M. S., and White, A. F.: Lithological influences on contemporary and long-term regolith weathering at the Luquillo Critical Zone Observatory, Geochim. Cosmochim. Ac., 196, 224–251, https://doi.org/10.1016/j.gca.2016.09.038, 2017.

555   Buytaert, W., De Bièvre, B., Wyseure, G., and Deckers, J.: The effect of land use changes on the hydrological behaviour of Histic Andosols in south Ecuador, Hydrol. Process., 19: 3985–3997, https://doi.org/10.1002/hyp.5867, 2005.

Buytaert, W., Deckers, J., and Wyseure, G.: Description and classification of nonallophanic Andosols in south Ecuadorian alpine grasslands (páramo), Geomorphology, 73, 207–221, https://doi.org/10.1016/j.geomorph.2005.06.012, 2006.

Canadell, J., Jackson, R. B., Ehleringer, J. B., Mooney, H. A., Sala, O. E., and Schulze, E. D.: Maximum rooting depth of

560   vegetation types at the global scale, Oecologia, 108, 583-595, https://doi.org/10.1007/BF00329030, 1996.

Carabajo-Hidalgo, A., Sabaté, S., Crespo, P., Asbjornsen, H.: Brief windows with more favorable atmospheric conditions explain patterns of Polylepis reticulata tree water use in a high-altitude Andean forest, Tree Physiology, 43(12), 2085–2097, https://doi.org/10.1093/treephys/tpad109, 2023.

Carrillo-Rojas, G., Silva, B., Rollenbeck, R. Célleri, R., and Bendix, J.: The breathing of the Andean highlands: Net ecosystem exchange and evapotranspiration over the páramo of southern Ecuador, Agr. Forest Meteorol, 265, 30-47, https://doi.org/10.1016/j.agrformet.2018.11.006, 2019.

Chadwick, O. A., Derry, L. A., Vitousek, P. M., Huebert, B. J., and Hedin, L. O.: Changing sources of nutrients during four million years of ecosystem development, Nature, 397, 491-497, https://doi.org/10.1038/17276, 1999.

Chadwick, O. A., Gavenda, R. T., Kelly, E. F., Ziegler, K., Olson, C. G., Elliott, W. C., and Hendricks, D. M.: The impact of climate on the biogeochemical functioning of volcanic soils, Chem. Geol., 202, 195-223, https://doi.org/10.1016/j.chemgeo.2002.09.001, 2003.

Clapuyt, F., Vanacker, V., Van Oost, K., 2016. Reproducibility of UAV-based earth topography reconstructions based on Structure-from-Motion algorithms. Geomorphology 260, 4–15. https://doi.org/10.1016/j.geomorph.2015.05.011.

Coblentz, D. and Keating, P. L.: Topographic controls on the distribution of tree islands in the high Andes of south-western Ecuador, Journal of Biogeography, 35, 2026-2038, https://doi.org/10.1111/j.1365-2699.2008.01956.x, 2008.

Comas, X., Terry, N., Hribljan, J. A., Erik Lilleskov, E., Suarez, E., Chimner, R. A., and Kolka, R.: Estimating belowground carbon stocks in peatlands of the Ecuadorian páramo using ground penetrating radar (GPR), J. Geophys. Res.-Biogeo., 122, 370-386, https://doi.org/10.1002/2016JG003550, 2017.

Cramer, M. D., Hoffmann, V., and Verboom, G. A.: Nutrient availability moderates transpiration in Ehrharta calycina, New Phytol., 179, 1048-1057, https://doi.org/10.1111/j.1469-8137.2008.02510.x, 2008.

Crawley, M. J.: The R book, John Wiley and Sons Limited, Chichester, UK, 2009.

Dawson, T. E., Hahm, W. J., and Crutchfield-Peters, K.: Digging deeper: what the critical zone perspective adds to the study of plant ecophysiology, New Phytol., 226, 666-671, https://doi.org/10.1111/nph.16410, 2020.

Delfim, J., Schoebitz, M., Paulino, L., Hirzel, J., and Zagal, E.: Phosphorus availability in wheat, in volcanic soils inoculated with phosphate-solubilizing Bacillus thuringiensis, Sustainability, 10, 144, https://doi.org/10.3390/su10010144, 2018.

Dixon, J. L., Chadwick, O. A., and Vitousek, P. M.: Climate-driven thresholds for chemical weathering in postglacial soils of New Zealand, J. Geophys. Res.-Earth Surf., 121, 1619-1634, https://doi.org/10.1002/2016JF003864, 2016.

Fan, Y., Miguez-Macho, G., Jobbágy, E. G., Jackson, R. B., and Otero-Casal, C.: Hydrologic regulation of plant rooting depth, P. Natl. Acad. Sci. USA, 114, 10572-10577, https://doi.org/10.1073/pnas.1712381114, 2017.

Food and Agriculture Organization, World reference base for soil resources 2006. A framework for international classification, correlation and communication. Rome: World Soil Resources. Reports No 103, FAO/ISRIC/IUSS, 2006.

Hansen, B. C., Rodbell, D., Seltzer, G., León, B., Young, K., and Abbott, M.: Late-glacial and Holocene vegetational history from two sites in the western Cordillera of southwestern Ecuador, Palaeogeogr. Palaeoecol., 194, 79–108, doi:10.1016/S0031-0182(03)00272-4, 2003.

Hasenmueller, E. A., Gu, X., Weitzman, J. N., Adams, T. S., Stinchcomb, G. E., Eissenstat, D. M., Drohan, P. J., Brantley, S. L., and Kaye, J. P.: Weathering of rock to regolith: The activity of deep roots in bedrock fractures, Geoderma, 300, 11-31, https://doi.org/10.1016/j.geoderma.2017.03.020, 2017.

Hedin, L. O., Vitousek, P. M., and Matson, P. A.: Nutrient losses over four million years of tropical forest development, Ecology, 84, 2231-2255, https://doi.org/10.1890/02-4066, 2003.

600 Hobbie, S. E.: Effects of plant-species on nutrient cycling, Trends Ecol. Evol., 7, 336-339, https://doi.org/10.1016/0169-5347(92)90126-V, 1992.

Hofhansl, F., Wanek, W., Drage, S., Huber, W., Weissenhofer, A., and Richter, A.: Topography strongly affects atmospheric deposition and canopy exchange processes in different types of wet lowland rainforest, Southwest Costa Rica. Biogeochemistry 106, 371–396, https://doi.org/10.1007/s10533-010-9517-3, 2011.

605 Hribljan, J. A., Suárez, E., Heckman, K. A., Lilleskov, E. A., and Chimner, R. A.: Peatland carbon stocks and accumulation rates in the Ecuadorian paramo, Wetlands Ecol. Manage., 24, 113-127, https://doi.org/10.1007/s11273-016-9482-2, 2016.

Hribljan, J.A., Hough, M., Lilleskov, E.A., Suarez, E., Heckman, K., Planas-Clarke, A.M., Chimner, R.A.: Elevation and temperature are strong predictors of long-term carbon accumulation across tropical Andean mountain peatlands. Mitig Adapt Strateg Glob Change 29, 1, https://doi.org/10.1007/s11027-023-10089-y, 2024

610 Jackson, R. B., Schenk, H. J., Jobbágy, E. G., Canadell, J., Colello, G. D., Dickinson, R. E., Field, C. B., Friedlingstein, P., Heimann, M., Hibbard, K., Kicklighter, D. W., Kleidon, A., Neilson, R. P., Parton, W. J., Sala, O. E., and Sykes, M. T.: Belowground consequences of vegetation change and their treatment in models, Ecological Applications, 10, 470-483, https://doi.org/10.1890/1051-0761(2000)010[0470:BCOVCA]2.0.CO;2, 2000.

Jackson, R. B., Banner, J. L., Jobbágy, E. G., Pockman, W. T., and Wall, D. H.: Ecosystem carbon loss with woody plant 615 invasion of grasslands, Nature, 418, 623-626, https://doi.org/10.1038/nature00910, 2002.

Jantz, N. and Behling, H.: A Holocene environmental record reflecting vegetation, climate, and fire variability at the Páramo of Quimsacocha, southwestern Ecuadorian Andes, Vegetation History and Archaeobotany., 21, 169-185, https://doi.org/10.1007/s00334-011-0327-x, 2012.

Jobbágy, E. G. and Jackson, R. B.: The distribution of soil nutrients with depth: Global patterns and the imprint of plants, 620 Biogeochemistry, 53, 51-77, https://doi.org/10.1023/A:1010760720215, 2001.

Jobbágy, E. G. and Jackson, R. B.: The uplift of soil nutrients by plants: Biogeochemical consequences across scales, Ecology, 85, 2380-2389, https://doi.org/10.1890/03-0245, 2004.

Jobbágy, E. G. and Jackson, R. B.: Groundwater and soil chemical changes under phreatophytic tree plantations, J. Geophys. Res.-Biogeo., 112, G02013, https://doi.org/10.1029/2006JG000246, 2007.

625 Kelly, E. F., Chadwick, O. A., and Hilinski, T. E.: The effects of plants on mineral weathering, Biogeochemistry, 42, 21-53, https://doi.org/10.1023/A:1005919306687, 1998.

Klute, A.: Water Retention: Laboratory Methods, in: Methods of Soil Analysis: Part 1 Physical and Mineralogical Methods, edited by: Klute, A., Soil Science Society of America, American Society of Agronomy, Madison, WI, USA, 635–662, https://doi.org/10.2136/sssabookser5.1.2ed.c26, 1986.

630 Kurniawan, S., Corre, M. D., Matson, A. L., Schulte- Bisping, H., Utami, S. R., van Straaten, O., and Veldkamp, E.: Conversion of tropical forests to smallholder rubber and oil palm plantations impacts nutrient leaching losses and nutrient retention efficiency in highly weathered soils, Biogeosciences, 15, 5131-5154, https://doi.org/10.5194/bg-15-5131-2018, 2018.

Landeweert, R., Hoffland, E., Finlay, R. D., Kuyper, T. W., and van Breemen, N.: Linking plants to rocks: ectomycorrhizal fungi mobilize nutrients from minerals, Trends Ecol. Evol., 16, 248-254, https://doi.org/10.1016/S0169-5347(01)02122-X,

635 2001.

Lazo, P.X., Mosquera, G.M., McDonnell, J.J., and Crespo, P.: The role of vegetation, soils, and precipitation on water storage and hydrological services in Andean páramo catchments, J. Hydrol., 572, 805-819, https://doi.org/10.1016/J, 2019.

Maher, K.: The role of fluid residence time and topographic scales in determining chemical fluxes from landscapes, Earth and Planetary Science Letters, 312(1–2), 48–58. https://doi.org/10.1016/j.epsl.2011.09.040, 2011.

640 Marín, F., Dahik, C., Mosquera, G., Feyen, J., Cisneros, P., and Crespo, P.: Changes in soil hydro-physical properties and SOM due to pine afforestation and grazing in Andean environments cannot be generalized, Forests, 10, 1-23, https://doi.org/10.3390/f10010017, 2018.

McLaughlin, S. B. and Wimmer, R.: Calcium physiology and terrestrial ecosystem processes, New Phytol., 142, 373-417, 1999.

645 Minaya, V., Corzo, G., Romero-Saltos, H., van der Kwast, J., Lantinga, E., Galárraga-Sánchez, R., and Mynett, A.: Altitudinal analysis of carbon stocks in the Antisana páramo, Ecuadorian Andes, Journal of Plant Ecology, 9, 553-563, https://doi.org/10.1093/jpe/rtv073, 2016.

Molina, A., Vanacker, V., Corre, M. D., and Veldkamp, E.: Patterns in soil chemical weathering related to topographic gradients and vegetation structure in a high Andean tropical ecosystem, J. Geophys. Res.-Earth Surf., 124, 666-685,

650 https://doi.org/10.1029/2018JF004856, 2019.

Mora, D. E. and Willems, P.: Decadal oscillations in rainfall and air temperature in the Paute River basin-southern Andes of Ecuador, Theoretical and Applied Climatology., 108, 267-282, https://doi.org/10.1007/s00704-011-0527-4, 2012.

Mosquera, P. V., Hampel, H., Vázquez, R. F., and Catalan, J.: Water chemistry variation in tropical high-mountain lakes on old volcanic bedrocks, Limnol. Oceanogr., 67, 1522–1536, https://doi.org/10.1002/lno.12099, 2022.

655 Nieminen, T. M., Derome, K., Meesenburg, H., and De Vos, B.: Chapter 16-Soil Solution: Sampling and Chemical Analyses, Developments in Environmental Science., 12, 301-315, https://doi.org/10.1016/B978-0-08-098222-9.00016-9, 2013.

Olshansky, Y., Knowles, J. F., Barron-Gafford, G. A., Rasmussen, C., Abramson, N., and Chorover, J.: Soil fluid biogeochemical response to climatic events, J. Geophys. Res.-Biogeo., 124, 2866-2882, https://doi.org/10.1029/2019JG005216, 2019.

660 Páez-Bimos, S., Villacís, M., Morales, O., Calispa, M., Molina, A., Salgado, S., De Bièvre, B., Muñoz, T., and Vanacker, V.: Vegetation effects on soil pore structure and hydraulic properties in volcanic ash soils of the high Andes, Hydrol., Process, 36, e14678, https://doi.org/10.1002/hyp.14678, 2022.

Páez-Bimos, S., Molina, A., Calispa, M., Dellmelle, P., Lahuatte, B., Villacís, M., Muñoz, T., and Vanacker, V.: Soil–vegetation–water interactions controlling solute flow and chemical weathering in volcanic ash soils of the high Andes, Hydrol.

665 Earth Syst. Sci, 27, 1507–1529, https://doi.org/10.5194/hess-27-1507-2023, 2023.

Ping, C.-L., Michaelson, G. J., Stiles, C. A., and González, G.: Soil characteristics, carbon stores, and nutrient distribution in eight forest types along an elevation gradient, eastern Puerto Rico. Ecological Bulletins, 54, 67–86, https://www.jstor.org/stable/26796806, 2013.

Podwojewski, P. and Poulenard, J.: En los suelos del páramo del Ecuador, Serie Páramo 5, GTP/Abya Yala, Quito, Ecuador,

670 ISBN: 9978-04-591-0, 2000.

Porder, S. and Chadwick, O. A.: Climate and soil-age constraints on nutrient uplift and retention by plants, Ecology, 90, 623-636, https://doi.org/10.1890/07-1739.1, 2009.

Poulenard, J., Podwojewski, P., and Herbillon, A. J.: Characteristics of non-allophanic andisols with hydric properties from the Ecuadorian paramos, Geoderma, 117, 267–281, https://doi.org/10.1016/s0016-7061(03)00128-9, 2003.

675 R Core Team: R: A language and environment for statistical computing, R Foundation for Statistical Computing, Vienna, Austria, https://www.R-project.org/, last access: 24 March 2023.

Rada, F., Azocar, A., and García-Nuñez, C.: Plant functional diversity in tropical Andean paramos, Plant Ecology and Diversity., 12, 539-553, https://doi.org/10.1080/17550874.2019.1674396, 2019.

Ramsay, P. M.: The Páramo Vegetation of Ecuador: the community ecology, dynamics and productivity of tropical grasslands

680 in the Andes, PhD thesis 1-274, University of Wales, UK, 1992.

Rempe, D. M. and Dietrich, W. E.: Direct observations of rock moisture, a hidden component of the hydrologic cycle, P. Natl. Acad. Sci. USA, 115, 2664-2669, https://doi.org/10.1073/pnas.1800141115, 2018.

Rodbell, D. T., Bagnato, S., Nebolini, J. C., Seltzer, G. O., and Abbott, M. B.: A Late-Glacial-Holocene tephrochronology for glacial lakes in southern Ecuador, Quaternary Research, 57, 343-354, https://doi.org/10.1006/qres.2002.2324, 2002.

685 Schenk, H. J. and Jackson, R. B.: Rooting depths, lateral root spreads and below-ground/above-ground allometries of plants in water-limited ecosystems, Journal of Ecology, 90, 480-494, https://www.jstor.org/stable/3072232, 2002.

Schwendenmann, L. and Veldkamp, E.: The role of dissolved organic carbon, dissolved organic nitrogen and dissolved inorganic nitrogen in a tropical wet forest ecosystem, Ecosystems, 8, 339-351, https://doi.org/10.1007/s10021-003-0088-1, 2005.

690 Shaul, O.: Magnesium transport and function in plants: the tip of the iceberg, Biometals, 15, 307-321, https://doi.org/10.1023/A:1016091118585, 2002.

Tenorio, G. E., Vanacker, V., Campforts, B., Álvarez, L., Zhiminaicela, S., Vercruysse, K., Molina, A., and Govers, G.: Tracking spatial variation in river load from Andean highlands to inter-Andean valleys, Geomorphology, 308, 175–189, https://doi.org/10.1016/j.geomorph.2018.02.009, 2018.

695   Tonneijck, F. H., Jansen, B., Nierop, K. G. J., Verstraten, J. M., Sevink, J., and de Lange, L.: Towards understanding of carbon stocks and stabilization in volcanic ash soils in natural Andean ecosystems of northern Ecuador, Eur. J. Soil Sci., 61, 392–405, https://doi.org/10.1111/j.1365-2389.2010.01241.x, 2010.

Tripler, C. E., Kaushal, S. S., Likens, G. E., and Walter, M. T.: Patterns in potassium dynamics in forest ecosystems, Ecology Letters, 9, 451-466, https://doi.org/10.1111/j.1461-0248.2006.00891.x, 2006.

700   Uhlig, D., Schuessler, J. A., Bouchez, J., Dixon, J. L., and von Blanckenburg, F.: Quantifying nutrient uptake as driver of rock weathering in forest ecosystems by magnesium stable isotopes, Biogeosciences, 14, 3111-3128, https://doi.org/10.5194/bg-14-3111-2017, 2017.

Uhlig, D., Amelung, W., and von Blanckenburg, F.: Mineral nutrients sourced in deep regolith sustain long-term nutrition of mountainous temperate forest ecosystems, Global Biogeochem. Cy., 34, e2019GB006513,

705   https://doi.org/10.1029/2019GB006513, 2020.

van Dam, J. C., Stricker, J. N. M., and Droogers, P.: Inverse method to determine soil hydraulic functions from multistep outflow experiments, Soil Sci. Soc. Am. J., 58(3), 647–652. https://doi.org/10.2136/sssaj1994.03615995005800030002x, 1994.

van Genuchten, M. T.: A closed-form equation for predicting the hydraulic properties of unsaturated soils, Soil Sci. Soc. Am.

710   J., 44, 892-898, 1980.

van Hoorn, J. W.: Determining hydraulic conductivity with the inversed auger hole and infiltrometer methods, Proceedings of the International Drainage Workshop, 150-249, International Institute for Land Reclamation and Improvement, Wageningen, the Netherlands, 1979.

Vitousek, P., Chadwick, O., Matson, P., Allison, S., Derry, L., Kettley, L., Luers, A., Mecking, E., Monastra, V., and Porder,

715   S.: Erosion and the Rejuvenation of Weathering-derived Nutrient Supply in an Old Tropical Landscape, Ecosystems, 6, 762-772, https://doi.org/10.1007/s10021-003-0199-8, 2003.

Vitousek, P. M. Nutrient Cycling and Limitation: Hawaii as a Model System. USA: Princeton University Press, ISBN: 0-691-11579-6, 2004.

White, A. F., Schulz, M. S., Stonestrom, D. A., Vivit, D. V., Fitzpatrick, J., Bullen, T. D., Maher, K., and Blum, A. E.: Chemical

720   weathering of a marine terrace chronosequence, Santa Cruz, California. Part II: Solute profiles, gradients and the comparisons of contemporary and long-term weathering rates, Geochim. Cosmochim. Acta, 73, 2769–2803, https://doi.org/10.1016/j.gca.2009.01.029, 2009.

White, A. F., Schulz, M. S., Vivit, D. V., Bullen, T. D., and Fitzpatrick, J.: The impact of biotic/abiotic interfaces in mineral nutrient cycling: a study of soils of the Santa Cruz chronosequence, California, Geochim. Cosmochim. Ac., 77, 62-85,

725   https://doi.org/10.1016/j.gca.2011.10.029, 2012.

White, S.: Grass páramo as hunter-gatherer landscape, The Holocene, 23, 898-915, https://doi.org/10.1177/0959683612471987, 2013.

Zhang, H., Aldana-Jague, E., Clapuyt, F., Wilken, F., Vanacker, V., Van Oost, K.: Evaluating the potential of post-processing kinematic (PPK) georeferencing for UAV- based structure-from-motion (SfM) photogrammetry and surface change detection. Earth Surf. Dynam. 7, 807–827. https://doi.org/10.5194/esurf-7-807-2019, 2019.